TIV Contrast Source Inversion of mCSEM data

T. Wiik ([1]), L. O. Løseth ([2]), B. Ursin ([1]), K. Hokstad ([1,2])

([1])Department for Petroleum Technology and Applied Geophysics, Norwegian University of Science and Technology

([2]) Statoil ASA

Summary

We present a Contrast Source Inversion (CSI) method for marine Controlled Source Electromagnetic (mCSEM) data in conductive media. The inversion is carried out with respect to electric conductivity in a medium which is transversely isotropic in the vertical direction (TIV). The method is demonstrated on field data which, in this case, shows that the TIV inversion is preferred over isotropic inversion in order to identify weak anomalies. The reason for this is that both the horizontal and vertical conductivity affects the signal propagation in the overburden, while the response from the main reservoir is dominated by the vertical conductivity alone.

Introduction

The use of mCSEM data in hydrocarbon prospecting is based on the assumption that hydrocarbon saturated formations possess a significantly lower electric conductivity compared to its surroundings. The EM field emitted from a controlled source travelling inside this resistive region will be less attenuated at far source/receiver offsets than the field propagating in water saturated formations, and the effect of such resistive areas should thus be recognizable at far offsets (Eidesmo et al., 2002). The interpretation of mCSEM data is not necessarily straightforward. In order to explain the recorded data, imaging algorithms that solve the inverse scattering problem of determining the subsurface parameters are helpful.

We apply the CSI method, based on an integral equation framework, extended to TIV media to the inversion of mCSEM data. Anisotropic effects are present in recorded mCSEM data, and the isotropic assumption may not be sufficient to give a realistic image of the subsurface. Thus, we consider media in which the horizontal and vertical conductivities may differ.

The isotropic method has been investigated in several other settings earlier; see for instance Abubakar and van den Berg (2004) and the references therein. The method introduces so called *contrast sources*, which may be interpreted as sources emitting signals that are really scattered from a scattering object, and regularization is introduced linearly into the cost functional. Based on these contrast sources we alternatingly minimize a cost functional with respect to the contrast sources and the contrast between the real medium and a chosen background medium. The final result is an estimate of the contrast, which describes the difference between the chosen background and the estimated medium.

When the method is applied to field data, the results show the importance of including anisotropy in the inversion and of considering the nature of the regularizer before performing the inversion. In the example considered here, we find that TIV inversion is superior to inverting for an isotropic model. This is because both the horizontal and vertical conductivities affect the field propagation in the overburden, while the response from the main reservoir is dominated by the vertical conductivity alone since it acts as a thin layer (Løseth and Ursin, 2007).

Methodology

We consider a background medium with electric conductivity, electric permittivity and magnetic permeability denoted by

$$\sigma_0 = \begin{pmatrix} \sigma_{0,h} & 0 & 0 \\ 0 & \sigma_{0,h} & 0 \\ 0 & 0 & \sigma_{0,v} \end{pmatrix}, \tag{1}$$

ε_0 and μ_0, where the subscript *0* denotes the background and the subscripts *h/v* denotes horizontal and vertical conductivities, respectively. In this background there is a finite domain D which contains an anomaly in electric conductivity. It is well known that when accepting Ohm's law, the electric field at points inside D satisfies (Abubakar and van den Berg, 2004)

$$E_i(x) = E_i^{inc}(x) + \int_D G_{ij}^E(x,x')\sigma_{0,v}(x')\chi_{jj}(x')E_j(x')dx' = E_i^{inc}(x) + G_{ij}^{E,D}W_j, \tag{2}$$

where the subscripts *i,j* denote the components, the superscript *inc* denotes the incident field from the source and G_{ij}^E denotes the electric Green's tensor. The contrast χ is given by

$$\chi = \begin{pmatrix} \frac{\sigma_h}{\sigma_{0,v}} - \frac{\sigma_{0,h}}{\sigma_{0,v}} & 0 & 0 \\ 0 & \frac{\sigma_h}{\sigma_{0,v}} - \frac{\sigma_{0,h}}{\sigma_{0,v}} & 0 \\ 0 & 0 & \frac{\sigma_v}{\sigma_{0,v}} - 1 \end{pmatrix}, \tag{3}$$

$G_{ij}^{E,D}$ is an integral operator and $W_j = \chi_{jj}E_j$ is the contrast source. The scattered electric and magnetic fields at receiver locations are correspondingly given by

$$\begin{aligned} f_i^E(x) &= \int_D G_{ij}^E(x,x')\sigma_{0,v}(x')\chi_{jj}(x')E_j(x')dx' = G_{ij}^{E,S}W_j, \\ f_i^H(x) &= \int_D G_{ij}^H(x,x')\sigma_{0,v}(x')\chi_{jj}(x')E_j(x')dx' = G_{ij}^{H,S}W_j. \end{aligned} \tag{4}$$

The solution to the CSI problem is defined as

$$\begin{aligned} \arg\min_{W_j^{k,l},\chi} & \alpha_1^E \sum_{k=1}^{N_f}\sum_{l=1}^{N_s} \left\| \Xi^{E,k,l}\left(f^{E,k,l} - G^{E,S,k}W^{k,l} \right) \right\|_S^2 + \alpha_1^H \sum_{k=1}^{N_f}\sum_{l=1}^{N_s} \left\| \Xi^{H,k,l}\left(f^{H,k,l} - G^{H,S,k}W^{k,l} \right) \right\|_S^2 + \\ & \alpha_2 \sum_{k=1}^{N_f}\sum_{l=1}^{N_s} \left\| \chi E^{inc,k,l} - W^{k,l} + \chi G^{E,D,k}W^{k,l} \right\|_D^2 + \lambda^2 \left\| \Xi_m\left(\chi - \chi^{ref} \right) \right\|_D^2, \end{aligned} \tag{5}$$

where N_f, N_s are the number of frequencies and sources, respectively. Ξ is the data weights and Ξ_m determines the model weights for the prior term, which are chosen as a second order smoothing filter in the example. Further, χ^{ref} is the prior model, which is chosen to be zero in the example to emphasize only a smooth reconstruction. The normalization constants are given by

$$\alpha_1^{E^{-1}} = \sum_{k=1}^{N_f}\sum_{l=1}^{N_s}\left\|\Xi^{E,k,l} f^{E,k,l}\right\|_S^2, \alpha_1^{H^{-1}} = \sum_{k=1}^{N_f}\sum_{l=1}^{N_s}\left\|\Xi^{H,k,l} f^{H,k,l}\right\|_S^2, \alpha_2^{-1} = \sum_{k=1}^{N_f}\sum_{l=1}^{N_s}\left\|\chi E^{inc,k,l}\right\|_D^2, \quad (6)$$

and λ is the regularization parameter. The minimization problem is solved as described in Abubakar and van den Berg (2004) using an alternating scheme. The cost functional is first minimized with respect to each of the contrast sources, before it is minimized with respect to the contrast itself to obtain an estimate for the conductivity inside D. This process is then repeated iteratively.

Results

The real dataset was collected over the Troll field in 2008. The survey was similar to the survey described in Farrelly et al. (2004), and the line crosses three laterally separated anomalies as shown in Figure 2 in Farrelly et al. (2004). The largest anomaly is the Troll West Gas Province (TWGP), but it also crosses the Troll West Oil Province (TWOP) further west, which lies slightly deeper and has less contrast. The inversion was carried out using frequencies 0.25Hz and 0.75Hz, as the fundamental frequency alone was not able to pick up the smaller anomalies. Further, the smaller anomalies only appeared after a sufficient level of data misfit was achieved. All receivers measured the inline electric and cross line magnetic fields. The background model consisted of a sea layer, with depth equal to the arithmetic mean of the receiver depths and conductivity 3.3 S/m, and a homogeneous half space with conductivity 0.35 S/m. Upon inspecting the seismic section the domain D was chosen as $-10000m \le x \le 12000m, -1000m \le y \le 1000m, 1000m \le z \le 2000m$ with grid size $\Delta x = 250m, \Delta y = 250m, \Delta z = 50m$. The background model overlaid a seismic section is shown in Figure 1, where the red boxes mark the approximate positions of the expected anomalies. The initial model was a 0.01S/m anomaly in the rightmost box in Figure 1.
Figures 2 and 3 show the isotropic and TIV inversion results, respectively. Figure 2 shows that the box to the right only has a small contrast in the isotropic case, while the large anomaly connected to TWGP is introduced at approximately the correct position. Figure 3(a) shows a nearly zero estimate for the horizontal contrast in the TIV inversion. This is as expected since the signal propagation in the reservoir is governed by the vertical conductivity (Løseth and Ursin, 2007), and thus when we apply a smoothing filter the profile for σ_h will be smoothed towards zero if the background is properly chosen. However, Figure 3(b) displays a brighter anomaly in σ_v than the isotropic result at the approximate position of the initial model, the large anomaly from TWGP is introduced, and even a small anomaly to the left of TWGP approximately at the position of the TWOP is visible. The large anomaly from the TIV inversion is however more spread out than the isotropic estimate. We observe a nice fit with the seismic section, although the small anomaly close to TWOP in Figure 3(b) is slightly too close to TWGP. This might be an effect due to the bias introduced by the smoothing regularization, which could also lead to questioning this anomaly.

Conclusions

We have demonstrated a CSI inversion method for mCSEM experiments in TIV anisotropic media. The method is based on an integral equation framework, and it relies on choosing an appropriate background model. The method is formulated as an optimization problem of minimizing a cost functional, and prior model information is introduced linearly into the cost functional. This may be used for numerical stabilization or structural information.
We found that the method is applicable to real field data, but information concerning the background model is needed for a good result. The method should thus be viewed in context with other methods in

which the entire survey area is discretized. In this example three anomalies are present in the TIV inversion, while only two are seen in the isotropic inversion. All the anomalies are brighter using TIV inversion, which is probably because both the horizontal and vertical conductivity affect the signal propagation in the overburden, while the response from the main reservoir is dominated by the vertical conductivity alone.

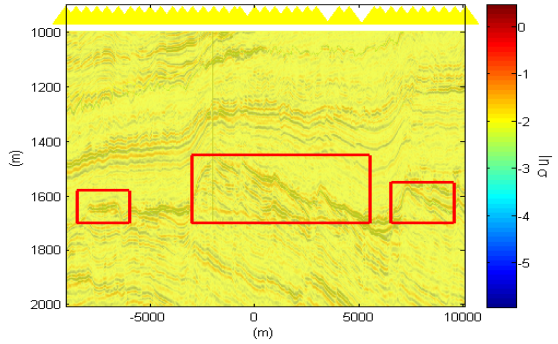

Figure 1: *Initial model.*

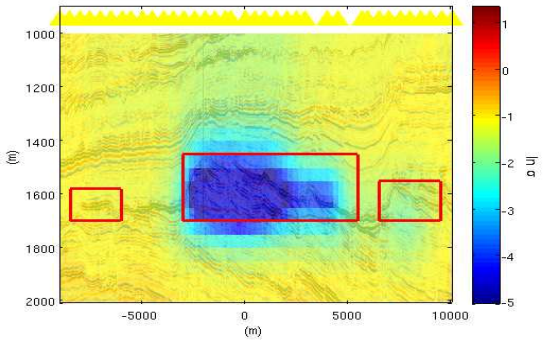

Figure 2: *Isotropic inversion.*

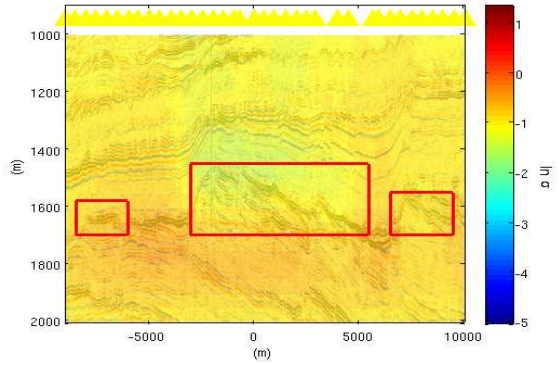

Figure 3(a): *TIV inversion,* σ_h.

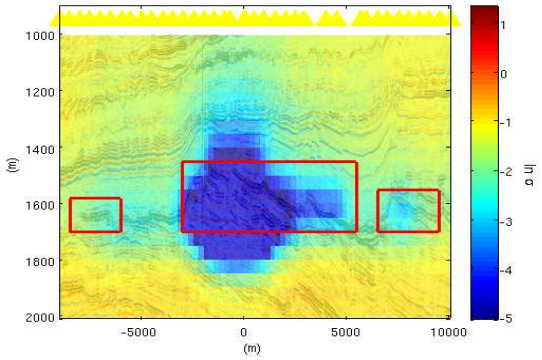

Figure 3(b): *TIV inversion,* σ_v.

Acknowledgements

The authors wish to thank the Troll license for permission to publish this work. Torgeir Wiik acknowledges Statoil ASA for sponsoring his Ph.D. project. Bjørn Ursin has received financial support from VISTA and from the Norwegian Research Council through the ROSE project.

References

Abubakar, A. and van den Berg, P.M. [2004] Iterative forward and inverse algorithms based on domain integral equations for three-dimensional electric and magnetic objects. *Journal of Computational Physics*, **195**, 236–262.

Eidesmo, T., Ellingsrud, S., MacGregor, L.M., Constable, S., Sinha, M.C., Johansen, S., Kong, F.N., and Westerdahl, H. [2002] Sea Bed Logging (SBL), a new method for remote and direct identification of hydrocarbon filled layers in deepwater areas. *First Break*, **20**, 144–152.

Farrelly, B., Ringstad, C., Johnstad, S.E., and Ellingsrud, S. [2004] Remote characterization of hydrocarbon filled reservoirs at the Troll field by sea bed logging. *EAGE Fall Research Workshop on Advances in Seismic Acquisition Technology*.

Løseth, L.O. and Ursin, B. [2007] Electromagnetic fields in planarly layered anisotropic media. *Geophysical Journal International*, **170**, 44–80.